Atmos. Chem. Phys. Discuss., 12, 9035–9077, 2012
www.atmos-chem-phys-discuss.net/12/9035/2012/
doi:10.5194/acpd-12-9035-2012

Atmospheric Chemistry and Physics Discussions

Carbon and hydrogen isotopic ratios of atmospheric methane in the upper troposphere over the Western Pacific

T. Umezawa[1,*], T. Machida[2], K. Ishijima[3], H. Matsueda[4], Y. Sawa[4], P. K. Patra[3], S. Aoki[1], and T. Nakazawa[1]

[1]Center for Atmospheric and Oceanic Studies, Graduate School of Science, Tohoku University, Sendai, Japan
[2]National Institute for Environmental Studies, Tsukuba, Japan
[3]Japan Agency for Marine-Earth Science and Technology, Yokohama, Japan
[4]Meteorological Research Institute, Tsukuba, Japan
[*]now at: Max Planck Institute for Chemistry, Mainz, Germany

Received: 8 March 2012 – Accepted: 21 March 2012 – Published: 10 April 2012

Correspondence to: T. Umezawa (taku.umezawa@mpic.de)

Published by Copernicus Publications on behalf of the European Geosciences Union.

Abstract

We present the mixing ratio, $\delta^{13}C$ and δD of atmospheric CH_4 using commercial aircraft in the upper troposphere (UT) over the Western Pacific for the period December 2005–September 2010. The observed results were compared with those obtained using commercial container ships in the lower troposphere (LT) over the same region. In the Northern Hemisphere (NH), the UT CH_4 mixing ratio shows high values in the boreal summer–autumn, when the LT CH_4 mixing ratio reaches a seasonal minimum. From tagged tracer experiments made using an atmospheric chemistry transport model, we found that such high CH_4 values are due to rapid transport of air masses influenced by CH_4 sources in South Asia and East Asia. The observed isotopic ratio data suggest that CH_4 sources in these areas have relatively low $\delta^{13}C$ and δD signatures, implying biogenic sources. Latitudinal distributions of the annual average UT and LT CH_4 mixing ratio intersect each other in the tropics; the mixing ratio value is lower in the UT than in the LT in the NH and the situation is reversed in the Southern Hemisphere (SH), due mainly to the NH air intrusion into the SH through the UT. Such intersection of the latitudinal distributions is observable in δD but not in $\delta^{13}C$, implying additional contribution of a reaction of CH_4 with active chlorine in the marine boundary layer. $\delta^{13}C$ and δD show low values in the NH and high values in the SH both in the UT and in the LT. We also observed an increase in the CH_4 mixing ratio and decreases in $\delta^{13}C$ and δD during 2007–2008 in the UT and LT over the Western Pacific, possibly due to enhanced biogenic emissions in the tropics and NH.

1 Introduction

Methane (CH_4) is an important trace gas in atmospheric chemistry and climate. CH_4 is emitted into the atmosphere from natural and anthropogenic sources, and it is destroyed mainly by a reaction with hydroxyl radical (OH) in the troposphere. Global average CH_4 budget is relatively well constrained (Patra et al., 2011), but there are still large

ACPD
12, 9035–9077, 2012

uncertainties in quantitative estimation of individual strengths and distributions (e.g., Forster et al., 2007). Ice core analyses revealed a rapid increase of atmospheric CH_4 in the industrial/agricultural era, due to anthropogenic CH_4 emissions (e.g., Nakazawa et al., 1993a; Etheridge et al., 1998). Systematic measurements of the atmospheric CH_4 mixing ratio were initiated in the late 1970s (Blake and Rowland, 1986), and they clarified that atmospheric CH_4 increased at rates of 10–20 parts per billion by volume (ppb = nmol mol^{-1}) per year in the 1980s, such an increase declined greatly in the early 1990s until the growth rate became nearly zero in 1999, and then the CH_4 mixing ratio began to increase again after 2007 (Dlugokencky et al., 2003, 2009; Rigby et al., 2008; Terao et al., 2011).

The atmospheric CH_4 mixing ratio has been observed mostly at surface baseline stations (e.g., Steele et al., 1987; Cunnold et al., 2002), and the data obtained were used to depict global picture of atmospheric CH_4 variations, as well as to constrain atmospheric chemistry transport models for estimation of global CH_4 budget (e.g., Fung et al., 1991; Bousquet et al., 2006; Patra et al., 2009). However, it is pointed out that the present observation network of atmospheric CH_4 is not sufficient for describing atmospheric CH_4 variations caused by regional sources (Fung et al., 1991; Chen and Prinn, 2006; Houweling et al., 2006; Bousquet et al., 2011). On the other hand, satellite observations can cover a spatially wide area. In fact, the data from the Scanning Imaging Absorption Spectrometer for Atmospheric Chartography (SCIAMACHY) aboard the ENVISAT satellite revealed the atmospheric CH_4 variations over such regions as Asia, Africa and South America where important CH_4 sources exist but direct atmospheric CH_4 observations are very sparse (Frankenberg et al., 2011). The data from SCIAMACHY were also used for an inverse modeling to improve our knowledge on distributions of CH_4 sources (Bergamaschi et al., 2007, 2009). CH_4 data by Greenhouse gases Observing SATellite (GOSAT) are also becoming available, which are likely to constrain surface emissions at weekly to monthly time intervals (Yoshida et al., 2011). Aircraft observations using a grab sampling with subsequent laboratory analysis are also helpful for high-precision measurements of the atmospheric CH_4 mixing ratio in

ACPD
12, 9035–9077, 2012

the upper troposphere (UT). However, regular measurements using chartered aircraft are expensive, so that number of observations for trace gases is limited (Nakazawa et al., 1993b; Francey et al., 1999; Miller et al., 2007).

Commercial airliners were also used for measurements of trace gases over a long distance especially in the UT. The Tohoku University group conducted trace gas observations on domestic and international flights by Toa Domestic Airlines (renamed Japan Air System later) and Japan Airlines (JAL) (Tanaka et al., 1983, 1987a; Nakazawa et al., 1991, 1993b; Ishijima et al., 2001, 2010). Observations of CO_2, CH_4 and CO in the UT over the Western Pacific were also conducted using JAL aircraft by the Meteorological Research Institute, Japan (Matsueda and Inoue, 1996; Matsueda et al., 1998, 2002). This observation program has been merged into a new project named CONTRAIL (Comprehensive Observation Network for TRace gases by AILiner) (Machida et al., 2008).

Regular measurements of trace gases using commercial aircraft are also made under the CARIBIC (Civil Aircraft for the Regular Investigation of the atmosphere Based on an Instrument Container) (Brenninkmeijer et al., 2007). This program reported an interesting phenomenon that the mixing ratios of greenhouse gases and nonmethane hydrocarbons are high in the UT (approximately 10–12 km) over South Asia during the Asian summer monsoon season of June–September (Shuck et al., 2010; Baker et al., 2011). Such high CH_4 mixing ratios were also found by satellite measurements (Park et al., 2004; Xiong et al., 2009). It is known that a substantial amount of CH_4 is emitted in the Asian region (South Asia, East Asia and Southeast Asia) from natural and anthropogenic sources, such as rice paddies, livestock, fossil fuel consumption and natural wetlands (Fung et al., 1991; Olivier and Berdowski, 2001; Yan et al., 2003; Yamaji et al., 2003). However, since systematic observations of the CH_4 mixing ratio in rapidly developing Asian countries, such as China and India, are still sparse (Lal et al., 2004; Zhou et al., 2004; Battacharya et al., 2009), quantitative understanding of CH_4 sources in this region is insufficient.

ACPD
12, 9035–9077, 2012

Carbon and hydrogen isotopic ratios of CH_4 ($\delta^{13}C$ and δD) are useful for distinguishing contributions of individual CH_4 sources to atmospheric CH_4 variations, since each source has its own characteristic signatures, the respective values of $\delta^{13}C$ and δD being about −60 and −300 ‰ for biogenic source, −40 and −180 ‰ for fossil fuel source, and −25 and −200 ‰ for biomass burning source (Quay et al., 1999). The number of their atmospheric observations has been increased since a continuous-flow measurement technique with a gas-chromatograph isotope ratio mass spectrometry (GC-IRMS) was available (Rice et al., 2001; Miller et al., 2002; Umezawa et al., 2009). Measurements of $\delta^{13}C$ are made at selected sites of the National Oceanic and Atmospheric Administration/Global Monitoring Division (NOAA/GMD) (Miller et al., 2002; Dlugokencky et al., 2009), Ny Ålesund, Svalbard (Morimoto et al., 2006), and two sites in the western part of the United States (Tyler et al., 2007). Tyler et al. (2007) also reported the measurement results of δD. However, their systematic observations are still limited, and only campaign-based observations were made for $\delta^{13}C$ and δD variations in the free troposphere (Sugawara et al., 1996; Tyler et al., 1999; Mak et al., 2000; Umezawa et al., 2011).

In order to understand spatial and temporal variations of $\delta^{13}C$ and δD in the UT over the Western Pacific, we analyzed the CONTRAIL air samples for these variables, in addition to the CH_4 mixing ratio. The results were compared with those observed in the lower troposphere (LT) using container ships that sailed on almost the same route as the CONTRAIL aircraft. We also made tagged tracer experiments using an atmospheric chemistry transport model to examine causes of the CH_4 variations observed in the UT. In this paper, we present the results obtained from our observation and model studies, and discuss them in terms of CH_4 sources and atmospheric transport.

ACPD
12, 9035–9077, 2012

2 Methods

2.1 Air sample collection

As part of the CONTRAIL project, an Automatic air Sampling Equipment (ASE) was installed on Boeing 747-400. Since details of air sampling using ASE have been described elsewhere (Machida et al., 2008; Matsueda et al., 2008), only a brief description is presented here. ASE consists of two packages and each package has six titanium sample flasks, so that 12 air samples can be collected during one flight. Each flask is cylindrical shape with solenoid valves at both ends and its inner volume is about 1.7 l. The sample air was collected using an air-conditioning system of the aircraft. The air sampling procedures at each location assigned before a flight were automatically performed by controlling a metal bellows pump and the solenoid valves using a specially designed control unit which receives flight information from a navigation system of the aircraft. Particles involved in the sample air were removed by using a sintered inline filter.

Figure 1 shows typical sampling locations of this study. The collection of air samples were made almost twice a month between Narita (NRT), Japan and Sydney (SYD) or Brisbane (BNE), Australia for December 2005–March 2009 and between NRT and Guam (GUM) for April 2009–March 2010, and once a month between NRT and Honolulu (HNL) for April–September 2010. The departure airport in Australia was frequently changed to BNE instead of SYD after October 2007, and the sample collection at 30° S was temporarily terminated after September 2008. Air samplings between NRT and SYD started again in April 2011 and ongoing.

We also analyzed the air samples taken onboard commercial container ships sailing between Tokyo, Japan and Sydney, or Auckland, New Zealand in about 40 days. Each air sample was collected into a 550 ml Pyrex glass flask at every 5° latitude, as shown in Fig. 1. Details of this observation program have been described elsewhere (Tanaka et al., 1987b; Nakazawa et al., 1992, 1997a; Morimoto et al., 2000; Ishijima et al., 2009; Yashiro et al., 2009).

ACPD
12, 9035–9077, 2012

2.2 Measurement of CH_4 mixing ratio

ASE filled with the air samples was returned to the National Institute for Environmental Studies (NIES), Tsukuba, Japan within a day from the sampling, and the mixing ratios of various trace gases including CH_4 were analyzed. The CH_4 mixing ratio of each air sample was determined against the NIES-94 CH_4 scale using a gas chromatograph (Agilent 5890, Agilent Technologies Inc.) equipped with a flame ionization detector (GC-FID) (Tohjima et al., 2002; Machida et al., 2008). On the other hand, the air samples collected onboard container ships were analyzed for the CH_4 mixing ratio relative to the Tohoku University (TU) 1988 scale (Aoki et al., 1992) using the GC-FID (Agilent 6890) installed at TU (Umezawa, 2009). The analytical precision of the GC-FID for the CH_4 mixing ratio was estimated to be less than 2.0 ppb for both institutes. The intercomparison of the NIES and TU scales showed that the two scales agree well with each other within the analytical precisions. We therefore applied no corrections to the mixing ratio data taken by the two institutes. It was also found, from the World Meteorological Organization (WMO)/Round Robin program for standards of greenhouse gases, that there are small differences of 2.1–2.6 ppb between the TU and WMO scales and of 3.5–4.6 ppb between the NIES and WMO scales in a mixing ratio range of 1750–1840 ppb (Zhou et al., 2009).

2.3 Measurements of $\delta^{13}C$ and δD

Aliquot of each ASE air sample was transferred into two evacuated 100 ml sample flasks at NIES, and the flasks were sent to TU for $\delta^{13}C$ and δD measurements. At TU, the air sample in each flask was further divided into two for duplicate analyses of $\delta^{13}C$ or δD. The air samples from container ships were also divided by the same procedure as above to allow duplicate analyses of $\delta^{13}C$ and δD.

Since details of our $\delta^{13}C$ and δD analyses, using a gas chromatograph combustion/pyrolysis isotope ratio mass spectrometer (GC-C/P-IRMS) have been reported (Umezawa et al., 2009), only a brief description is presented here. The air sample in the

ACPD
12, 9035–9077, 2012

100 ml flask was flushed by pure helium into a CH_4 preconcentration trap containing HayeSep D maintained at −130 °C and then warmed to −83 °C to release simultaneously trapped gases such as N_2. The trapped CH_4 was transferred into a cryofocusing trap (CP-PoraBOND Q) kept at −196 °C. The concentrated CH_4 was released into a PoraPLOT Q column for separation from the residual gas components. Then CH_4 was combusted into CO_2 at 940 °C or pyrolyzed into H_2 at 1450 °C for the subsequent continuous flow mass spectrometer measurements of $\delta^{13}C$ and δD, respectively, using ThermoQuest/Finnigan Delta Plus XP. The analytical precision was estimated to be 0.08 ‰ for $\delta^{13}C$ and 2.2 ‰ for δD. $\delta^{13}C$ and δD values in this study are reported relative to the international standards of the Vienna Peedee Belemnite (V-PDB) and the Vienna Standard Mean Ocean Water (V-SMOW), respectively.

To verify the long-term stability of our $\delta^{13}C$ and δD measurements, we analyzed aliquot of "test gas" at least twice on every measurement day. The test gas is dry natural air in a 47 l aluminum cylinder. The CH_4 mixing ratio, $\delta^{13}C$ and δD of the test gas were determined to be (1876 ± 1.1) ppb, (−47.07 ± 0.06) ‰ and (−98.8 ± 2.1) ‰, respectively. Measured $\delta^{13}C$ value of the test gas was stable to be (−47.12 ± 0.10) ‰ from the starting date of our measurement until April 2008. Afterward, the measured value was shifted to (−46.85 ± 0.09) ‰. The cause is still unclear, since we had not change any measurement settings. To keep data consistency, we added −0.27 ‰ to the measured values after the gap. With regard to the stability of our δD measurements, measured values determined by our GC-C/P-IRMS system are dependent on the pyrolysis condition (Umezawa et al., 2009). Bock et al. (2010) inspected the pyrolysis condition of their similar measurement system in detail. Using the average measured value of the test gas on each measurement day, the assigned value of our working standard (pure H_2) was corrected so that the δD value of the test gas should be constant.

Analyses of the CH_4 mixing ratio were made for all air samples collected from the aircraft and container ships, while $\delta^{13}C$ and δD were analyzed for selected samples, since their analyses are time-consuming. Although the air sampling with ASE was made twice a month between NRT and SYD or BNE and between NRT and GUM,

ACPD
12, 9035–9077, 2012

one of the two sets of samples was analyzed for each month. The air samples were collected onboard the container ships every 5° latitude, but the isotope analysis was made on the samples at almost 10° latitude interval.

2.4 Data analysis

To extract a long-term trend and a seasonal cycle from temporally discrete data of the CH_4 mixing ratio, $\delta^{13}C$ and δD, a digital filtering technique (Nakazawa et al., 1997b) was applied. The technique consists of stepwise calculation process involving linear interpolation, Reinsch-type cubic splines, Fourier harmonics and a Butterworth filter. In this study, the Butterworth filter with a cutoff period of 24 months was used to derive the long-term trend, and the average seasonal cycle was expressed by fundamental and its first harmonics. Signals with periods of 4–24 months, obtained by further applying the Butterworth filter with a cutoff period of 4 months, were defined as short-term variations. The best-fit curve to the observed data was obtained by summing the long-term trend, the average seasonal cycle and the short-term variations.

Since the numbers of $\delta^{13}C$ and δD data taken in the LT are limited, we classified them into five latitudinal bands of 35°–25° N, 20°–10° N, 5° N–10° S, 15°–25° S and 30°–40° S (Fig. 1) and then applied the curve fitting to the data sets of the respective bands. These latitude bands were determined by carefully inspecting the observed seasonal cycles of the CH_4 mixing ratio at individual sampling latitudes, so that the seasonal features are similar within each band. On the other hand, the curve fitting method was simply applied to individual UT data sets at the assigned sampling latitudes.

2.5 Tagged tracer simulations

To examine where the CH_4 sources contributing to CH_4 variations in the UT are located, we made tagged tracer experiments using the CCSR (Center for Climate System Research)/NIES/FRCGC (Frontier Research Center for Global Change) Atmospheric General Circulation Model-based Chemistry Transport Model (ACTM) for CH_4 mixing

ACPD
12, 9035–9077, 2012

ratio (Patra et al., 2009). In order to discriminate CH_4 emitted from different source regions, the original surface flux field was divided into 15 regions on the globe (Table 1), and each CH_4 tracer is simulated separately with each flux field. We confirmed that sum of the 15 tracers and the simulated mixing ratio with original flux field agreed with each other within 0.1 %. The original surface CH_4 fluxes were prepared by multiplying optimal scaling factors to natural/biogenic emissions from the Goddard Institute for Space Studies (GISS) (Fung et al., 1991; Matthews and Fung, 1987), as well as to anthropogenic/industrial emissions from the Emission Database for Global Atmospheric Research (EDGER) inventory (Olivier and Berdowski, 2001). It was assumed that atmospheric CH_4 is destroyed by reacting with OH, Cl and $O(^1D)$ during transport, and the mixing ratios of the reactants were adopted from independent modeling results (Sudo et al., 2002; Takigawa et al., 1999). The model meteorological field was nudged to Japanese 25-yr ReAnalysis (JRA25) (Onogi et al., 2007). Patra et al. (2009) showed that the CH_4 mixing ratio variations observed at surface baseline sites around the world are reproduced relatively well by using this model. In their model simulations, the natural emissions and loss due to chemical reactions varied seasonally but their seasonality was repeated year after year, anthropogenic CH_4 emissions for each year were derived by interpolating or extrapolating the EDGAR inventories, and the model meteorology was interannually variable. The hourly model outputs were sampled for the times and locations specified by our observations, to compare directly with the observational results.

3 Results and discussions

3.1 Variations of atmospheric CH_4 and its isotopes in the UT

Figure 2 shows time series of the CH_4 mixing ratio, $\delta^{13}C$ and δD obtained in the UT between NRT and Australia (SYD or BNE) and between NRT and GUM. At 32°–15° N, high CH_4 mixing ratios often appear in boreal summer–autumn, and relatively low CH_4

ACPD
12, 9035–9077, 2012

mixing ratios are found in winter–spring (Fig. 3a). The summer–autumn CH_4 mixing ratios are higher by as much as 30–80 ppb than the winter–spring mixing ratios. The low CH_4 mixing ratios observed in winter–spring may be partly attributable to an intrusion of stratospheric air with low CH_4 mixing ratios into the troposphere (e.g., Sugawara et al., 1997). A similar phenomenon was also found for the N_2O mixing ratio at 32° N from the same ASE samples (Ishijima et al., 2010). In general, $\delta^{13}C$ and δD show a weak negative correlation with the CH_4 mixing ratio; high and low values of $\delta^{13}C$ and δD are observable in winter–spring and autumn, respectively (Figs. 3b and 3c).

There are some studies that observed the summer–autumn high CH_4 mixing ratios in the UT of the NH mid-latitudes. Matsueda and Inoue (1996) reported, from their CH_4 measurements in the UT between Cairns, Australia and NRT during 1993–1994, that in boreal autumn, high CH_4 mixing ratios appear in the NH, but the feature disappears with going southward. Schuck et al. (2010) also found high CH_4 mixing ratios in the UT around 20°–40° N in eastern South Asia during June–September 2008. Furthermore, the Atmospheric Infrared Sounder (AIRS) instrument onboard the EOS/Aqua satellite observed high CH_4 mixing ratios at 150–300 hPa levels over northern South Asia for July–September with maximum in an early September (Xiong et al., 2009). Measurements over geographically wide area were made by the Halogen Occultation Experiment (HALOE) instrument onboard the Upper Atmosphere Research Satellite (UARS) spacecraft (Park et al., 2004), and their results revealed that high CH_4 mixing ratios appear at 136 hPa level at 10°–40° N during June–September, especially in South Asia. These previous studies suggest that boundary layer air affected by various CH_4 sources in the Asian region is transported into the UT and responsible for the high CH_4 mixing ratios in summer.

The high CH_4 mixing ratio values observed in the NH in boreal summer–autumn become unclear with going southward, and in the tropics, the CH_4 mixing ratios shows slightly high and low values in boreal winter–spring and summer–autumn, respectively (Figs. 2e–h and Fig. 3a). The peak-to-peak amplitude of the seasonal CH_4 cycle is about 30 ppb at 10° N and 5° N and 15 ppb at the equator and 6° S, indicating

ACPD
12, 9035–9077, 2012

a southward reduction of the seasonal cycle of CH_4 fluxes. In the SH, the seasonal CH_4 cycles are much reduced, and its seasonal minimum and maximum appear in the austral summer (December–January) and spring (September–October), respectively (Fig. 3a). The CH_4 seasonality observed in the SH-UT is generally consistent with that observed using aircraft over Cape Grim, Australia (Francey et al., 1999), as well as with zonal-mean seasonal cycle reported from satellite observations (Park et al., 2004). It should be noted that Ishijima et al. (2010) found the low N_2O mixing ratios at 30° S in the austral spring, due to an intrusion of the stratospheric air into the UT, but the limited number of stratospheric samples affects insignificantly on the seasonal CH_4 cycle at the latitude.

While $\delta^{13}C$ and δD vary seasonally in opposite phase with the CH_4 mixing ratio in the NH (32°–10° N), their seasonal cycles are rather irregular in the tropics (5° N and the equator), resulting in a less tight negative correlation with the CH_4 mixing ratio in the southern low latitude (6° S). It is seen in the SH (13°–30° S) that $\delta^{13}C$ and δD show a weak negative correlation with the CH_4 mixing ratio in some places, but both variables are independent on the CH_4 mixing ratio as a whole.

3.2 Comparisons of the CH_4 variations in the UT with that in the LT

To interpret variations of the CH_4 mixing ratio, $\delta^{13}C$ and δD in the UT, we compare them with those observed in the LT. The CH_4 mixing ratio, $\delta^{13}C$ and δD observed in the UT at 21° N are compared in Fig. 4a with those observed in the LT at 20°–10° N. As clearly seen in this figure, the UT- and LT-CH_4 mixing ratios vary seasonally in opposite phase. It is also seen in summer that the CH_4 mixing ratio is often higher in the UT than in the LT. The summertime minimum CH_4 mixing ratio is commonly found at surface baseline sites in northern mid-latitudes, due to a CH_4 + OH reaction enhanced in summer (e.g., Dlugokencky et al., 1994; Patra et al., 2009). The OH density is higher in the LT than in the UT as a whole, but its seasonal change should occur in the almost same phase throughout the troposphere (e.g., Spivakovsky et al., 2000). Therefore, the summertime

ACPD
12, 9035–9077, 2012

high CH_4 mixing ratios observed in the UT suggest an overwhelming role of transport of air masses that are strongly influenced by some CH_4 sources.

The CH_4 + OH reaction leads to an enrichment in ^{13}C and D of atmospheric CH_4 through the kinetic isotope effect (KIE) (e.g., Saueressig et al., 2001). As seen in Fig. 4a, $\delta^{13}C$ and δD show high values in boreal summer in the NH-LT, corresponding to the seasonal minimum of the CH_4 mixing ratio, which is similar to the results obtained at other NH mid-latitude sites (Quay et al., 1991, 1999; Miller et al., 2002; Tyler et al., 2007). $\delta^{13}C$ and δD also vary seasonally in the UT, but their phases are almost opposite to those in the LT. This phase difference also supports that the summertime CH_4 values in the NH-UT is significantly affected by CH_4 sources rather than the CH_4+OH reaction. Considering that the summertime $\delta^{13}C$ and δD values are often lower in the UT than in the LT, CH_4 sources with low $\delta^{13}C$ and δD would influence on the seasonal CH_4 cycle in the UT.

Figure 4b shows temporal variations of the CH_4 mixing ratio, $\delta^{13}C$ and δD in the tropical UT (the equator) and LT (5° N–10° S). The UT- and LT-CH_4 mixing ratios vary almost in phase, showing the seasonal maximum and minimum in boreal winter and summer, respectively. This would be caused by the fact that the tropical tropospheric air is vertically well mixed due to strong convection. For the seasonal CH_4 cycle observed in the tropical LT, seasonally dependent air transport would be particularly important, as pointed out by Nakazawa et al. (1997a) and Yashiro et al. (2009); the observation area is usually covered by the NH air with high CH_4 mixing ratios, but the air with low CH_4 mixing ratios comes from the SH in boreal summer in association with Asian monsoon.

Variations of $\delta^{13}C$ and δD should also be affected by the seasonally different air transport mentioned above. In general, $\delta^{13}C$ and δD are low in the NH-LT, increase going southward, and are almost constant in the SH-LT (Quay et al., 1999; Miller et al., 2002). Our latitudinal distributions of $\delta^{13}C$ and δD in the LT, which will be presented later (Fig. 5), also show similar features. Therefore, it is expected that the transport of the NH (SH) air through the LT deplete (enrich) ^{13}C and D of atmospheric CH_4 in the

ACPD
12, 9035–9077, 2012

tropics. In fact, the seasonal cycles of $\delta^{13}C$ and δD observed in the LT of the tropics are generally interpretable in this context (Fig. 4b).

The results observed at 24° S in the UT and 15°–25° S in the LT are shown in Fig. 4c. As seen in this figure, the SH-CH_4 mixing ratio is higher in the UT than in the LT throughout the year. Nakazawa et al. (1991) and Matsueda et al. (2002) found in the SH that annual-average CO_2 mixing ratios are higher in the UT than in the LT, which is also shown by a large number of in-situ CO_2 data taken by CONTRAIL flights (Sawa et al., 2012). Such CO_2 increase with altitude in the SH is ascribed to the interhemispheric transport through the tropical UT (Miyazaki et al., 2008; Sawa et al., 2012). Similar vertical distributions of the CH_4 mixing ratio were reported from aircraft measurements over Cape Grim (Francey et al., 1999). The CH_4 mixing ratios obtained in this study show similar seasonal cycles in the LT and UT. In this connection, Francey et al. (1999) reported that the seasonal CH_4 cycles obtained at three levels between 0–8 km proceed in similar phase with that at the surface. Since no strong CH_4 sources exist around the Western Pacific region of the SH, the seasonal CH_4 cycle could be predominantly produced by the seasonality of the CH_4+OH reaction (Dlugokencky et al., 1994) as well as seasonal change of atmospheric transport of the NH air through the UT, as observed in the CO_2 mixing ratio (Sawa et al., 2012).

The $\delta^{13}C$ and δD values are relatively lower in the UT than in the LT in the SH. As described earlier, the abovementioned air mass transport from the NH into the SH through the UT is responsible for this difference. In this connection, the NH air has lower $\delta^{13}C$ and δD values than the SH air (see Fig. 5). By inspecting the seasonal cycle, it was found that both $\delta^{13}C$ and δD showed a negative correlation with the CH_4 mixing ratio in the LT, while such a relation is less obvious in the UT (Fig. 2i–l). The CH_4+OH reaction is a major CH_4 sink that contributes to the seasonal $\delta^{13}C$ and δD cycles through the KIE, yielding a negative correlations between the isotopic ratios and the CH_4 mixing ratio. Another possible factor that contributes to the $\delta^{13}C$ seasonality is a CH_4+Cl reaction (e.g., Allan et al., 2001, 2005), which has larger KIE than the CH_4+OH reaction (Saueressig et al., 1995; Tyler et al., 2000). Although the CH_4+OH

ACPD
12, 9035–9077, 2012

reaction is effective in the whole troposphere, the CH_4+Cl reaction is important only in the marine boundary layer (Allan et al., 2005). The Cl reaction has no strong impact on δD, because the hydrogen KIE of the Cl reaction is not significantly large compared to the major OH reaction (Saueressig et al., 1996; Tyler et al., 2000).

3.3 Latitudinal and annual changes

3.3.1 Latitudinal distribution in the UT and LT

Figure 5 shows the latitudinal distributions of annual averages of the CH_4 mixing ratio, $\delta^{13}C$ and δD in the UT and LT for the period 2007–2009. The UT distributions for 2007–2008 and 2009 were derived from the data taken between NRT and SYD or BNE and between NRT and GUM, respectively. In the LT, the CH_4 mixing ratio is high in the NH and decreases going southward until the value is almost constant in the extratropical SH. The CH_4 mixing ratio in the northernmost latitude band is about 100 ppb higher than the value in the extratropical SH. Such a latitudinal distribution of the CH_4 mixing ratio has been reported from the global baseline network (Dlugokencky et al., 1994), attributing the cause to the fact that a large portion of CH_4 source is located in the NH (e.g., Fung et al., 1991). The UT-CH_4 mixing ratio is higher in the NH than in the SH, but the north-south gradient in the UT (about 45 ppb) is smaller than that in the LT. It is also seen from Fig. 5 that the latitudinal distributions of the CH_4 mixing ratio in the UT and LT cross each other in the tropics; the CH_4 mixing ratio is lower in the UT than in the LT in the NH, and vice versa in the SH. Such latitudinal distributions are due to CH_4 emissions from the NH surface as well as to the NH air intrusion into the SH through the UT. A similar distribution feature has been reported for the CO_2 mixing ratio from measurements on the same flight route as this study (Nakazawa et al., 1991; Matsueda et al., 2002), more frequent and wider coverage measurements of the CONTRAIL project (Sawa et al., 2012) and global-scale simulations (Miyazaki et al., 2008).

ACPD
12, 9035–9077, 2012

In the LT, $\delta^{13}C$ increases with decreasing latitude from the NH to the tropics and the values are almost constant in the extratropical SH. A similar distribution has been reported from surface and shipboard measurements (Quay et al., 1991, 1999; Miller et al., 2002). The observed north-south gradient of $\delta^{13}C$ arises from the process that a large amount of CH_4 is emitted in the NH from biogenic sources with low $\delta^{13}C$ such as wetlands, rice paddies and ruminant animals and ^{13}C of atmospheric CH_4 is enriched by the OH reaction during southward transport (Miller et al., 2002). The north-south gradient of $\delta^{13}C$ is also found in the UT, but it is less pronounced than that in the LT. Compared with $\delta^{13}C$ in the LT, the UT value is almost equal in the NH and the tropics and lower in the SH. As a result, $\delta^{13}C$ does not show any clear intersection of the latitudinal distributions in the LT and UT. These profiles without intersection suggest that in addition to the NH air intrusion, some other factors contribute to the observed $\delta^{13}C$ distributions. As described above, the CH_4+Cl reaction could enrich ^{13}C significantly by its large KIE in the marine boundary layer, but it has only a minor effect on the destruction of atmospheric CH_4 (Allan et al., 2007). Since the present observations in the LT were made just above the open sea in the Western Pacific, our $\delta^{13}C$ values in the LT could be enriched significantly by the Cl reaction over the whole observation latitudes, resulting in the profiles without intersection between the LT and UT.

In the LT, δD shows almost the same latitudinal distributions as $\delta^{13}C$. The latitudinal distribution of δD was also measured by Quay et al. (1999) and Rice et al. (2001) using ships in the eastern Pacific, but their measurements are not systematic. The north-south gradient of δD in the LT can be interpreted in terms of unevenly distributed CH_4 sources in the NH and the SH, as well as the KIE by the OH reaction. The north-south gradient of δD is also apparent in the UT, although it is less pronounced than in the LT. Compared with δD in the LT, the UT value is lower and higher in the NH and the SH, respectively, yielding a intersection of the UT and LT latitudinal δD distributions, as was found in the CH_4 mixing ratio. A possible cause of the intersection is ascribed to the NH air intrusion into the SH through the UT. The Cl reaction also affects on δD in

ACPD
12, 9035–9077, 2012

the LT, but its effect would be minor, since the reaction does not have a large impact on δD (Saueressig et al., 1996; Tyler et al., 2000).

3.3.2 Recent increase of atmospheric CH_4

As seen in Fig. 5, the average CH_4 mixing ratio is increased by about 10 ppb at 30°–40° S, 15°–25° S, 5° N–10° S and 20°–10° N and by 17 ppb at 35°–25° N in the LT from 2007 to 2008. The mixing ratio increase between 2008 and 2009 is about 5 ppb at all latitude bands. Such increases of the mixing ratio are consistent with the results from baseline measurements (Dlugokencky et al., 2009; Terao et al., 2011). On the other hand, the respective decreases in δ^{13}C and δD between 2007 and 2008 are about 0.05 ‰ and 0.6 ‰ in the SH and the tropics (30°–40° S to 5° N–10° S) and by about 0.10 ‰ and 1.2 ‰ at NH mid-latitudes (20°–10° N and 35°–25° N), showing slightly more prominent decrease in the NH than in the tropics and SH. Such temporal decreases in δ^{13}C and δD suggest that the CH_4 mixing ratio increase was caused by enhanced emissions of isotopically light CH_4 from biogenic sources such as wetlands and rice paddies. For the period 2008–2009, the decrease in δ^{13}C is small (< 0.04 ‰) at all latitudes covered by this study, and δD shows (< 1 ‰) positive or negative changes, depending on the latitudes.

The CH_4 mixing ratio in the UT is increased by about 7 ppb in the tropics (13° S–10° N) and by about 15 ppb in the extratropics of both hemispheres between 2007 and 2008. On the other hand, δ^{13}C and δD decrease slightly by 0.03 ‰ and 1.2 ‰, respectively, at all latitudes covered by this study, but such decreases are not clearly dependent on the latitude. In this connection, it was pointed out that CH_4 emissions from the tropics are rapidly transported into the UT due to active convection and therefore could be hardly captured at existing surface baseline sites (Houweling et al., 2006; Bousquet et al., 2011).

Summarizing, increase of the CH_4 mixing ratio was observable for the period 2007–2008 in the LT and UT at our observation latitudes, accompanied by the δ^{13}C and δD

ACPD
12, 9035–9077, 2012

decreases, and they were more prominent in the NH. Enhanced CH_4 emissions in the tropics as well as boreal regions might explain these observed changes. At the same time, biogenic sources depleted in ^{13}C and D, such as wetlands and rice paddies, would be responsible for the observed CH_4 increase with decrease of $\delta^{13}C$ and δD.

Rigby et al. (2008) and Sasakawa et al. (2010) found high temperature anomalies in Siberia in 2007, suggesting that CH_4 emissions from boreal wetlands would have been enhanced. By using a two-dimensional box model with possible changes in OH, Rigby et al. (2008) indicated that the CH_4 increase in 2007 is attributable to CH_4 emissions enhanced in the NH. Dlugokencky et al. (2009) also suggested an enhancement of CH_4 emissions from boreal wetlands, resulting in the largest CH_4 increase in the Arctic and low $\delta^{13}C$ values at northern high-latitude site Alert, Canada, in late summer of 2007. On the other hand, Bousquet et al. (2011) indicated from their atmospheric inversion modeling that tropical wetlands are the major contributor to the CH_4 increase in 2007, also with a potential contribution from boreal wetlands.

3.4 Summertime elevated CH_4 in the UT of the NH

3.4.1 Tagged tracer results

To examine causes of the high CH_4 mixing ratios observed in the NH-UT in summer, we made tagged tracer experiments using the ACTM. Figure 6 shows the comparison of the observed and model-simulated CH_4 mixing ratios for the UT at 32°–15° N. As seen in this figure, the model reproduces the observed variations relatively well, especially for the appearance timing of high CH_4 mixing ratios. The tagged tracers for the respective regions are also shown in Fig. 6. As clearly seen in this figure, Regions 5 (South Asia) and Region 6 (East Asia) play an important role in the CH_4 variations in the NH-UT. The contribution of South Asia is larger than that of East Asia as a whole, and both regions are closely related to the high CH_4 mixing ratios in boreal summer–autumn, CH_4 from South Asia and East Asia being important for September–October and May–September, respectively. Such high CH_4 mixing ratios would be due to a rapid upward

ACPD
12, 9035–9077, 2012

transport of the boundary layer air by Asian summer monsoon (Jiang et al., 2007; Park et al., 2009; Xiong et al., 2009; Schuck et al., 2010). A sensitivity test, in which the model was run with and without seasonally varying sources, also indicated that enhanced vertical transport over these two regions predominantly drives the summertime high CH_4 mixing ratio peaks in the UT. It should be also noted that the CH_4 emission from rice paddies used in the model reaches a maximum around August–September in South Asia and June in East Asia.

It is also found from Fig. 6 that the differences between the observed and simulated CH_4 mixing ratios become larger after 2008. Since our model reproduces the appearance timing of the observed CH_4 peaks relatively well, the meteorological field and CH_4 source distributions would be plausibly incorporated into the model. Therefore, the large differences between the simulated and observed CH_4 mixing ratios after 2008 could be caused by insufficient temporal change in CH_4 sources in the model.

3.4.2 Isotopic signatures of CH_4 sources in South Asia and East Asia

Figure 7 shows plots of $\delta^{13}C$ and δD against the reciprocal of the CH_4 mixing ratio for the UT at 15°–32° N. This kind of plot is called as Keeling plot and often used to estimate the isotopic ratio of a source that exchanges a trace gas with the atmosphere (e.g., Pataki et al., 2003). In the light of the results of the tagged tracer experiments, we categorized the observed data into three regions of South Asia, East Asia and the rest of the world (hereafter referred to as baseline). The air samples categorized into the two regions have extremely high values of the corresponding tagged tracers for the respective regions, which exceed the average plus one standard deviation calculated for the observation period. The South Asian and East Asian samples were found in May–October with only one exception (December). It is obvious from Fig. 7 that air originated in South Asia and East Asia has higher CH_4 mixing ratios and lower $\delta^{13}C$ and δD than those of the baseline air. The average CH_4 mixing ratios are (1819 ± 28) and (1827 ± 26) ppb for the South-Asian and East-Asian air, respectively, while the mixing ratio value of the baseline air is (1796 ± 22) ppb, and the respective average

ACPD
12, 9035–9077, 2012

values of δ^{13}C and δD are (−47.08 ± 0.11) and (−90.3 ± 4.1) ‰ for South Asia and (−47.01 ± 0.11) and (−90.5 ± 3.9) ‰ for East Asia, while the corresponding values are (−46.96 ± 0.11) and (−87.3 ± 3.6) ‰ for the baseline air. Such high CH_4 mixing ratios and low isotopic values imply that CH_4 sources with lower δ^{13}C and δD relative to atmospheric CH_4 exist in both regions.

If is it assumed that CH_4 is emitted into the atmosphere from a single CH_4 source, the isotopic ratio of that source can be inferred as an intercept of the regression line for the Keeling plot. Our data yield δ^{13}C of (−52.8 ± 1.8) (correlation coefficient R = 0.68) and δD of (−359 ± 49) ‰ (R = 0.84) for South Asia, and δ^{13}C of (−53.8 ± 1.2) (R = 0.84) and δD of (−318 ± 42) ‰ (R = 0.83) for East Asia. These values suggest substantial contributions from biogenic CH_4 sources depleted in ^{13}C and D, such as rice paddies and livestock, to the summertime CH_4 sources in these regions. The model CH_4 flux has summertime enhanced rice emissions in both regions, which is generally consistent with isotopic signatures estimated in this study. The above assumption is usually valid for the atmosphere close to the source, such as in the forest canopy (e.g., Pataki et al., 2003) and the boundary layer (e.g., Llyod et al., 2001; Umezawa et al., 2011), but our measurements were made in the UT. Therefore, it should be noted that the sampled air would be influenced not only by CH_4 sources but also by chemical destructions and air mixing during its transport.

3.5 Longitudinal variations in the UT of the NH

Figure 8 shows longitudinal distributions of the CH_4 mixing ratio, δ^{13}C and δD in the UT between NRT and HNL. As seen in this figure, the CH_4 mixing ratios observed in May 2010 are extremely low between 160°–180° E, with the minimum value of 1655 ppb around 170° E. Such low CH_4 mixing ratios were not observable in the UT between NRT and SYD or BNE and between NRT and GUM (Fig. 2). The air samples with low CH_4 mixing ratios show high values of δ^{13}C and δD. To examine the cause, we analyzed the Japan Meteorological Agency Climate Data Assimilation System (JCDAS) reanalysis

ACPD
12, 9035–9077, 2012

data (Onogi et al., 2007), following the same method as used in Sawa et al. (2008), in which potential vorticity (PV) in PV-units (PVU = 10^{-6} km^2 kg^{-1} s^{-1}) was adopted as a measure of stratospheric air. By inspecting the PV distribution along the flight route, we found that the stratospheric air (> 3 PVU) intruded into the UT around 160°–180° E. It is known that the CH_4 mixing ratio decreases rapidly with increasing altitude in the stratosphere (e.g., Sugawara et al., 1997). Sugawara et al. (1997), Rice et al. (2003) and Röckmann et al. (2011) also found that stratospheric CH_4 is isotopically more enriched in ^{13}C and D than tropospheric CH_4. Regarding the air samples collected around 160°–180° E, the N_2O mixing ratios in the corresponding air samples were also lower than those of the other samples, due to the influence of stratospheric air.

Another interesting feature is that relatively high CH_4 mixing ratios, accompanied by low $\delta^{13}C$ and δD values, are observed in September 2010. As mentioned above, the observations in the NH-UT between NRT and SYD or BNE and between NRT and GUM indicate that the CH_4 mixing ratio is high in this season of the year (Fig. 2a–d), due to CH_4 from South Asia and East Asia. Observed longitudinal distributions showed the eastward decrease of the CH_4 mixing ratio and increase of $\delta^{13}C$ and δD in the east of the CH_4 maximum at 170° E, probably due to CH_4 outflow from South Asia and East Asia.

4 Conclusions

To elucidate temporal and spatial variations of the CH_4 mixing ratio, $\delta^{13}C$ and δD in the UT over the Western Pacific, air samples collected using the CONTAIL were analyzed. In the NH, the CH_4 mixing ratio showed high values in boreal summer, accompanied by relatively low $\delta^{13}C$ and δD values. By comparing with the LT data obtained using container ships in the same region, it was found in the NH that the CH_4 mixing ratios was higher in the UT than in the LT in summer. From the tagged tracer experiments, we found that CH_4 sources in South Asia and East Asia play an important role in the

ACPD
12, 9035–9077, 2012

summertime high CH_4 mixing ratio values in the NH-UT. The observed data of $\delta^{13}C$ and δD also suggested that biogenic CH_4 sources depleted in ^{13}C and D such as rice paddies and livestock contribute substantially to the high CH_4 mixing ratios observed in the NH-UT.

The latitudinal distributions of the CH_4 mixing ratio and δD in the LT and UT were found to intersect each other in low latitudes; the CH_4 mixing ratio and δD are higher and lower, respectively, in the LT than in the UT in the NH, and the situation is reversed in the SH. On the other hand, $\delta^{13}C$ showed similar values in the LT and UT of the NH, but the value is higher in the LT than in the UT in the SH. These latitudinal distributions can be interpreted mainly in terms of the NH air intrusion into the SH through the UT, but the CH_4+Cl reaction in the marine boundary layer may also affect the $\delta^{13}C$ distributions to some extent. Our data also indicate that the CH_4 mixing ratio has increased again since 2007, due to emissions of isotopically light biogenic CH_4 in the tropics and northern latitudes.

The analyses of $\delta^{13}C$ and δD in combination with the CH_4 mixing ratio are very useful for a better understanding of the global CH_4 cycle. However, their systematic measurements are still quite sparse. To examine their spatiotemporal variations in more detail, long-term measurements of these variables over a geographically wide area are further required. Modeling studies based on $\delta^{13}C$ and δD as well as the CH_4 mixing ratio are also necessary for quantitatively elucidating the CH_4 cycle, as well as for estimating the CH_4 budget.

Acknowledgement. We are grateful to Japan Airlines (JAL), JAL foundation and JAMCO for supporting the CONTRAIL project. We also appreciate Hachiuma Steamship CO. Ltd., NYK Line, NYK shipmanagement Pte. Ltd., and staffs of container ships for their cooperation in collecting air samples. Our thanks are due to K. Katsumata and H. Sandanbata, NIES and F. Arai and J. Miyakozawa, Tohoku University for their CH_4 mixing ratio analyses.

ACPD
12, 9035–9077, 2012

References

Allan, W., Manning, M. R., Lassey, K. R., Lowe, D. C., and Gomez, A. J.: Modeling the variation of $\delta^{13}C$ in atmospheric methane: phase ellipses and the kinetic isotope effect, Global Biogeochem. Cy., 15, 467–481, 2001.

Allan, W., Lowe, D. C., Gomez, A. J., Struthers, H., and Brailsford G. W.: Interannual variation of ^{13}C in tropospheric methane: implications for a possible atomic chlorine sink in the marine boundary layer, J. Geophys. Res., 110, D11306, doi:10.1029/2004JD005650, 2005.

Allan, W., Struthers, H., and Lowe, D. C.: Methane carbon isotope effects caused by atomic chlorine in the marine boundary layer: global model results compared with Southern Hemisphere measurements, J. Geophys. Res., 112, D04306, doi:10.1029/2006JD007369, 2007.

Aoki, S., Nakazawa, T., Murayama, S., and Kawaguchi, S.: Measurements of atmospheric methane at the Japanese Antarctic Station, Syowa, Tellus B, 44, 273–281, 1992.

Baker, A. K., Schuck, T. J., Slemr, F., van Velthoven, P., Zahn, A., and Brenninkmeijer, C. A. M.: Characterization of non-methane hydrocarbons in Asian summer monsoon outflow observed by the CARIBIC aircraft, Atmos. Chem. Phys., 11, 503–518, doi:10.5194/acp-11-503-2011, 2011.

Bergamaschi, P., Frankenberg, C., Meirink, J. F., Krol, M., Dentener, F., Wagner, T., Platt, U., Kaplan, J. O., Körner, S., Heimann, M., Dlugokencky, E. J., and Goede, A.: Satellite chartography of atmospheric methane from SCIAMACHY on board ENVISAT: 2. Evaluation based on inverse model simulations, J. Geophys. Res., 112, D2304, doi:10.1029/2006JD007268, 2007.

Bergamaschi, P., Frankenberg, C., Meirink, J. F., Krol, M., Villani, M. G., Houweling, S., Dentener, F., Dlugokencky, E. J., Miller, J. B., Gatti, L. V., Engel, A., and Levin, I.: Inverse modeling of global and regional CH_4 emissions using SCIAMACHY satellite retrievals, J. Geophys. Res., 114, D22301, doi:10.1029/2009JD012287, 2009.

Bhattacharya, S. K., Borole, D. V., Francey, R. J., Allison, C. E., Steele, L. P., Krummel, P., Langenfelds, R., Masarie, K. A., Tiwari, Y. K., and Patra, P. K.: Trace gases and CO_2 isotope records from Cabo de Rama, India, Curr. Sci., 97, 1336–1344, 2009.

Blake, D. R. and Rowland, F. S.: World-wide increase in tropospheric methane, 1978–1983, J. Atmos. Chem., 4, 43–62, 1986.

Bock, M., Schmitt, J., Behrens, M., Möller, L., Schneider, R., Sapart, C., and Fischer, H.: A gas chromatography/pyrolysis/isotope ratio mass spectrometry system for high-precision

ACPD
12, 9035–9077, 2012

δD measurements of atmospheric methane extracted from ice cores, Rapid Commun. Mass Spectrom., 24, 621–633, 2010.

Bousquet, P., Ciais, P., Miller, J. B., Dlugokencky, E. J., Hauglustaine, D. A., Prigent, C., Van der Werf, G. R., Peylin, P., Brunke, E.-G., Carouge, C., Langenfelds, R. L., Lathière, J., Papa, F., Ramonet, M., Schimidt, M., Steele, L. P., Tyler, S. C., and White, J.: Contribution of anthropogenic and natural sources to atmospheric methane variability, Nature, 443, 439–443, doi:10.1038/nature05132, 2006.

Bousquet, P., Ringeval, B., Pison, I., Dlugokencky, E. J., Brunke, E.-G., Carouge, C., Chevallier, F., Fortems-Cheiney, A., Frankenberg, C., Hauglustaine, D. A., Krummel, P. B., Langenfelds, R. L., Ramonet, M., Schmidt, M., Steele, L. P., Szopa, S., Yver, C., Viovy, N., and Ciais, P.: Source attribution of the changes in atmospheric methane for 2006–2008, Atmos. Chem. Phys., 11, 3689–3700, doi:10.5194/acp-11-3689-2011, 2011.

Brenninkmeijer, C. A. M., Crutzen, P., Boumard, F., Dauer, T., Dix, B., Ebinghaus, R., Filippi, D., Fischer, H., Franke, H., Frieß, U., Heintzenberg, J., Helleis, F., Hermann, M., Kock, H. H., Koeppel, C., Lelieveld, J., Leuenberger, M., Martinsson, B. G., Miemczyk, S., Moret, H. P., Nguyen, H. N., Nyfeler, P., Oram, D., O'Sullivan, D., Penkett, S., Platt, U., Pupek, M., Ramonet, M., Randa, B., Reichelt, M., Rhee, T. S., Rohwer, J., Rosenfeld, K., Scharffe, D., Schlager, H., Schumann, U., Slemr, F., Sprung, D., Stock, P., Thaler, R., Valentino, F., van Velthoven, P., Waibel, A., Wandel, A., Waschitschek, K., Wiedensohler, A., Xueref-Remy, I., Zahn, A., Zech, U., and Ziereis, H.: Civil Aircraft for the regular investigation of the atmosphere based on an instrumented container: the new CARIBIC system, Atmos. Chem. Phys., 7, 4953–4976, doi:10.5194/acp-7-4953-2007, 2007.

Chen, Y.-H. and Prinn, R. G.: Estimation of atmospheric methane emissions between 1996 and 2001 using a three-dimensional global chemical transport model, J. Geophys. Res., 111, D10307, doi:10.1029/2005JD006058, 2006.

Cunnold, D. M., Steele, L. P., Fraser, P. J., Simmonds, P. G., Prinn, R. G., Weiss, R. F., Porter, L. W., O'Doherty, S., Langenfelds, R. L., Krummel, P. B., Wang, H. J., Emmons, L., Tie, X. X., and Dlugokencky, E. J.: In situ measurements of atmospheric methane at GAGE/AGAGE sites during 1985–2000 and resulting source inferences, J. Geophys. Res., 107, 4225, doi:10.1029/2001JD001226, 2002.

Dlugokencky, E. J., Steele, L. P., Lang, P. M., and Masarie, K. A.: The growth rate and distribution of atmospheric methane, J. Geophys. Res., 99, 17021–17043, 1994.

ACPD

12, 9035–9077, 2012

Dlugokencky, E. J., Houweling, S., Bruhwiler, L., Masarie, K. A., Lang, P. M., Miller, J. B., and Tans, P. P.: Atmospheric methane levels off: temporary pause or a new steady-state?, Geophys. Res. Lett., 30, 1992, doi:10.1029/2003GL018126, 2003.

Dlugokencky, E. J., Bruhwiler, L., White, J. W. C., Emmons, L. K., Novelli, P. C., Montzka, S. A., Masarie, K. A., Lang, P. M., Crotwell, A. M., Miller, J. B. and Gatti, L. V.: Observational constraints on recent increases in the atmospheric CH_4 burden, Geophys. Res. Lett., 36, L18803, doi:10.1029/2009GL039780, 2009.

Etheridge, D. M., Steel, L. O., Francey, R. J., and Langenfelds, R. L.: Atmospheric methane between 1000 AD and present: evidence of anthropogenic emissions and climatic variability, J. Geophys. Res., 103, 15979–15993, 1998.

Forster, P., Ramaswamy, V., Artaxo, P., Berntsen, T., Betts, R., Fahey, D. W., Haywood, J., Lean, J., Lowe, D. C., Myhre, G., Nganga, J., Prinn, R., Raga, G., Schulz, M., and Dorland R. V.: Changes in Atmospheric Constituents and in Radiative Forcing, Climate Change 2007: The Physical Science Basis. Contribution of Working Group I to the Fourth Assessment Report of the Intergovernmental Panel on Climate Change, edited by: Solomon, S., Qin, D., Manning, M., Chen, Z., Marquis, M., Averyt, K. B., Tignor, M., and Miller, H. L., Cambridge, UK and New York, NY, USA, Cambridge University Press, 2007.

Francey, R. J., Steele, L. P., Langenfelds, R. L., and Pak, B. C.: High precision long-term monitoring of radiatively active and related trace gases at surface sites and from aircraft in the Southern Hemisphere atmosphere, J. Atmos. Sci., 56, 279–85, 1999.

Frankenberg, C., Aben, I., Bergamaschi, P., Dlugokencky, E. J., van Hees, R., Houweling, S., van der Meer, P., Snel, R., and Tol, P.: Global column-averaged methane mixing ratios from 2003 to 2009 as derived from SCIAMACHY: trends and variability, J. Geophys. Res., 116, D04302, doi:10.1029/2010JD014849, 2011.

Fung, I., John, J., Lerner, J., Mattews, E., Prather, M., Steele, L. P., and Fraser, P. J.: Three-dimensional model synthesis of the global methane cycle, J. Geophys. Res., 96, 13033–13065, 1991.

Houweling, S., Röckmann, T., Aben, I., Keppler, F., Krol, M., Meirink, J. F., Dlugokencky, E. J., and Frankenberg, C.: Atmospheric constraints on global emissions of methane from plants, Geophys. Res. Lett., 33, L15821, doi:10.1029/2006GL026162, 2006.

Ishijima, K., Nakazawa, T., Sugawara, S., Aoki, S., and Saeki, T.: Concentration variations of tropospheric nitrous oxide over Japan, Geophys. Res. Lett., 28(1), 171–174, 2001.

ACPD
12, 9035–9077, 2012

Ishijima, K., Nakazawa, T., and Aoki, S.: Variations of atmospheric nitrous oxide concentration in the Northern and Western Pacific, Tellus B, 61, 408–415, 2009.

Ishijima, K., Patra, P. K., Takigawa, M., Machida, T., Matsueda, H., Sawa, Y., Steele, L. P., Krummel, P. B., Langenfelds, R. L., Aoki, S., and Nakazawa, T.: Stratospheric influence on the seasonal cycle of nitrous oxide in the troposphere as deduced from aircraft observations and model simulations, J. Geophys. Res., 115, D20308, doi:10.1029/2009JD013322, 2010.

Jiang, J. H., Livesey, N. J., Su, H., Neary, L., McConnell, J. C., and Richards, N. A. D.: Connecting surface emissions, convective uplifting, and long-range transport of carbon monoxide in the upper troposphere: new observations from the Aura Microwave Limb Sounder, Geophys. Res. Lett., 34, L18812, doi:10.1029/2007GL030638, 2007.

Lal, S., Chand, D., Venkataramani, S., Appu, K. S., Naja, M., and Patra, P. K.: Trends in methane and sulfur hexafluoride at a tropical coastal site, Thumba (8.6° N, 77° E), in India, Atmos. Environ., 38, 1145–1151, 2004.

Lloyd, J., Francey, R. J., Mollicone, D., Raupach, M. R., Sogachev, A., Arneth, A., Byers, J. N., Kelliher, F. M., Rebmann, C., Valentini, R., Wong, S.-C., Bauer, G., and Schulze, E.-D.: Vertical profiles, boundary layer budgets, and regional flux estimates for CO_2 and its $^{13}C/^{12}C$ ratio and for water vapor above a forest/bog mosaic in central Siberia, Global Biogeochem. Cy., 15, 267–284, 2001.

Machida, T., Matsueda, H., Sawa, Y., Nakagawa, Y., Hirotani, K., Kondo, N., Goto, K., Nakazawa, T., Ishikawa, K., and Ogawa, T.: Worldwide measurements of atmospheric CO_2 and other trace gas species using commercial airlines, J. Atmos. Ocean. Tech., 25, 1744–1754, 2008.

Mak, J. E., Manning, M. R., and Lowe, D. C.: Aircraft observations of $\delta^{13}C$ of atmospheric methane over the Pacific in August 1991 and 1993: evidence of an enrichment in $^{13}CH_4$ in the Southern Hemisphere, J. Geophys. Res., 105, 1329–1335, 2000.

Matsueda, H. and Inoue, H. Y.: Measurements of atmospheric CO_2 and CH_4 using a commercial airliner from 1993 to 1994, Atmos. Environ., 30, 1647–1655, 1996.

Matsueda, H., Inoue, H. Y., Sawa, Y., Tsutsumi, Y., and Ishii, M.: Carbon monoxide in the upper troposphere over the Western Pacific between 1993 and 1996, J. Geophys. Res., 103, 19093–19110, 1998.

Matsueda, H., Inoue, H. Y., and Ishii, M.: Aircraft observations of carbon dioxide at 8–13 km altitude over the Western Pacific from 1993 to 1999, Tellus B, 54, 1–21, 2002.

ACPD
12, 9035–9077, 2012

Matsueda, H., Machida, T., Sawa, Y., Nakagawa, Y., Hirotani, K., Ikeda, H. Kondo, N., and Goto, K.: Evaluation of atmospheric CO_2 measurements from new flask air sampling of JAL airliner observations, Pap. Meteorol. Geophys., 59, 1–17, 2008.

Matthews, E. and Fung, I.: Methane emission from natural wetlands: global distirbution, area, and environmental characteristics of sources, Global Biogeochem. Cy., 1, 61–86, 1987.

Miller, J. B., Mack, K. A., Dissly, R., White, J. W. C., Dlugokencky, E. J., and Tans, P. P.:, Development of analytical methods and measurements of $^{13}C/^{12}C$ in atmospheric CH_4 from the NOAA Climate Monitoring and Diagnostics Laboratory Global Air Sampling Network, J. Geophys. Res., 107, 4178, doi:10.1029/2001JD000630, 2002.

Miller, J. B., Gatti, L. V., d'Amelio, M. T. S., Crotwell, A. M., Dlugokencky, E. J., Bakwin, P., Artaxo, P., and Tans, P. P.: Airborne measurements indicate large methane emissions from the Eastern Amazon basin, Geophys. Res. Lett., 34, L10809, doi:10.1029/2006GL029213, 2007.

Miyazaki, K., Patra, P. K., Takigawa, M., Iwasaki, T., and Nakazawa. T.: Global-scale transport of carbon dioxide in the troposphere, J. Geophys. Res, 113, D15301, doi:10.1029/2007JD009557, 2008.

Morimoto, S., Nakazawa, T., Higuchi, K., and Aoki, S.: Latitudinal distribution of atmospheric CO_2 sources and sinks inferred by $\delta^{13}C$ measurements from 1985 to 1991, J. Geophys. Res., 105, 24315–24326, 2000.

Morimoto, S., Aoki, S., Nakazawa, T., and Yamanouchi, T.: Temporal variations of the carbon isotopic ratio of atmospheric methane observed at Ny Ålesund, Svalbard from 1996 to 2004, Geophys. Res. Lett., 33, L01807, doi:10.1029/2005GL024648, 2006.

Nakazawa, T., Miyashita, K., Aoki, S., and Tanaka, M.: Temporal and spatial variations of upper tropospheric and lower stratospheric carbon dioxide, Tellus B, 43, 106–117, 1991.

Nakazawa, T., Murayama, S., Miyashita, K., Aoki, S., and Tanaka, M.: Longitudinally different variations of lower tropospheric carbon dioxide concentrations over the North Pacific Ocean, Tellus B, 44, 161–172, 1992.

Nakazawa, T., Machida, T., Tanaka, M., Fujii, Y., Aoki, S., and Watanabe, O.: Differences of the atmospheric CH_4 concentration between the Arctic and Antarctic regions in pre-industrial/pre-agricultural era, Geophys. Res. Lett., 20, 943–946, 1993a.

Nakazawa, T., Morimoto, S., Aoki, S., and Tanaka, M.: Time and space variations of the carbon isotopic ratio of tropospheric carbon dioxide over Japan, Tellus B, 45, 258–274, 1993b.

ACPD
12, 9035–9077, 2012

Nakazawa, T., Morimoto, S., Aoki, S., and Tanaka, M.: Temporal and spatial variaitions of the carbon isotopic ratio of atmospheric carbon dioxide in the Western Pacific region, J. Geophys. Res., 102, 1271–1285, 1997a.

Nakazawa, T., Ishizawa, M., Higuchi, K., and Trivett, N. B. A.: Two curve fitting methods applied to CO_2 flask data, Environmetrics, 8, 197–218, 1997b.

Olivier, J. G. J. and Berdowski, J. J. M.: Global emissions sources and sinks, in: The Climate System, edited by: Berdowski, J., Guicherit, R. and Heij, B. J., Lisse, The Netherlands, A. A. Balkema Publishers/Swets & Zeitlinger Publishers, 33–78, 2001.

Onogi, K., Tsutsui, J., Koide, H., Sakamoto, M., Kobayashi, S., Hatsushika, H. Matsumoto, T., Yamazaki, N., Kamahori, H., Takahashi, K., Kadokura, S., Wada, K. Kato, K., Oyama, R., Ose, T., Mannoji N., and Taira, R.: The JRA-25 Reanalysis, J. Meteorol. Soc. Jpn., 85, 369–432, 2007.

Park, M., Randel, W. J., Kinnison, D. E., Garcia, R. R., and Choi, W.: Seasonal variation of methane, water vapor, and nitrogen oxides near the tropopause: sattelite observations and model simulations, J. Geophys. Res., 108, D03302, doi:10.1029/2003JD003706, 2004.

Park, M., Randel, W. J., Emmons, L. K., and Liversey, N. J.: Transport pathways of carbon monoxide in the Asian summer monsoon diagnosed from MOZART, J. Geophys. Res., 114, D08303, doi:10.1029/2008JD010621, 2009.

Pataki, D. E., Ehleringer, J. R., Flanagan, L. B., Yakir, D., Bowling, D. R., Still, C. J., Buchmann, N., Kaplan, J. O., and Berry, J. A.: The application and interpretation of Keeling plots in terrestrial carbon cycle research, Global Biogeochem. Cy., 17, 1022, doi:10.1029/2001GB001850, 2003.

Patra, P. K., Takigawa, M., Ishijima, K., Choi, B.-C., Cunnold, D., Dlugokencky, E. J., Fraser, P., Gomez-Pelaez, A. J., Goo, T.-Y., Kim, J.-S., Krummel, P. Langenfelds, R., Meinhardt, F., Mukai, H., O'Doherty, S., Prinn, R. G., Simmonds, P., Steele, P., Tohjima, Y., Tsuboi, K., Uhse, K., Weiss, R., Worthy, D., and Nakazawa, T.: Growth rate, seasonal, synoptic and diurnal variations in lower atmospheric methane and its budget, J. Meteorol. Soc. Jpn., 87, 635–663, doi:10.2151/jmsj.87.635, 2009.

Patra, P. K., Houweling, S., Krol, M., Bousquet, P., Belikov, D., Bergmann, D., Bian, H., Cameron-Smith, P., Chipperfield, M. P., Corbin, K., Fortems-Cheiney, A., Fraser, A., Gloor, E., Hess, P., Ito, A., Kawa, S. R., Law, R. M., Loh, Z., Maksyutov, S., Meng, L., Palmer, P. I., Prinn, R. G., Rigby, M., Saito, R., and Wilson, C.: TransCom model simulations of CH_4 and related species: linking transport, surface flux and chemical loss with CH_4 variability in the tro-

ACPD
12, 9035–9077, 2012

posphere and lower stratosphere, Atmos. Chem. Phys., 11, 12813–12837, doi:10.5194/acp-11-12813-2011, 2011.
Quay, P. D., King, S. L., Stutsman, J., Wilbur, D. O., Steele, L. P., Fung, I., Gammon, R. H., Brown, T. A., Farwell, G. W., Grootes P. M., and Schmidt, F. H.: Carbon isotopic composition of atmospheric CH_4: fossil and biomass burning strengths, Global Biogeochem. Cy., 5, 25–47, 1991.
Quay, P., Stutsman, J., Wilbur, D., Snover, A., Dlugokencky, E., and Brown, T.: The isotopic composition of atmospheric methane, Global Biogeochem. Cy., 13, 445–461, 1999.
Rice, A. L., Gotoh, A. A., Ajie, H. O., and Tyler, S. C.: High-precision continuous-flow measurement of $\delta^{13}C$ and δD of atmospheric CH_4, Anal. Chem., 73, 4104–4110, 2001.
Rice, A. L., Tyler, S. C., McCarthy, M. C., Boering, K. A., and Atlas, E.: Carbon and hydrogen isotopic compositions of stratospheric methane: 1. High-precision observations from the NASA ER-2 aircraft, J. Geophys. Res., 108, 4460, doi:10.1029/2002JD003042, 2003.
Rigby, M., Prinn, R. G., Fraser, P. J., Simmonds, P. G., Langenfelds, R. L., Huang, J., Cunnold, D. M., Steele, L. P., Krummel, P. B., Weiss, R. F., O'Doherty, S., Salameh, P. K., Wang, H. J., Harth, C. M., Mühle, J., and Porter, L. W.: Renewed growth of atmospheric methane, Geophys. Res. Lett., 35, L22805, doi:10.1029/2008GL036037, 2008.
Röckmann, T., Brass, M., Borchers, R., and Engel, A.: The isotopic composition of methane in the stratosphere: high-altitude balloon sample measurements, Atmos. Chem. Phys., 11, 13287-13304, doi:10.5194/acp-11-13287-2011, 2011.
Sasakawa, M., Shimoyama, K., Machida, T., Tsuda, N., Suto, H., Arshinov, M., Davydov, D., Fofonov, A., Krasnov, O., Saeki, T., Koyama, Y., and Maksyutov, S.: Continuous measurements of methane from a tower network over Siberia, Tellus, 62, 403–416, 2010.
Saueressig, G., Bergamaschi, P., Crowley, J. N., Fischer, H., and Harris, G. W.: Carbon kinetic isotope effect in the reaction of CH_4 with Cl atoms, Geophys. Res. Lett., 22, 1225–1228, 1995.
Saueressig, G., Bergamaschi, P., Crowley, J. N., Fischer, H., and Harris, G. W.: D/H kinetic isotope effect in the reaction CH_4 + Cl, Geophys. Res. Lett., 23, 3619–3622, 1996.
Saueressig, G., Crowley, J. N., Bergamaschi, P., Brühl, C., Brenninkmeijer, C. A. M., and Fischer, H.: Carbon 13 and D kinetic isotope effects in the reactions of CH_4 with $O(^1D)$ and OH: new laboratory measurements and their implications for the isotopic composition of stratospheric methane, J. Geophys. Res., 106, 23127–23138, 2001.

ACPD
12, 9035–9077, 2012

Sawa, Y., Machida, T., and Matsueda, H.: Seasonal variations of CO_2 near the tropopause observed by commercial aircraft, J. Geophys. Res., 113, D23301, doi:10.1029/2008JD010568, 2008.

Sawa, Y., Machida, T., and Matsueda. H.: Aircraft observation of the seasonal variation in the transport of CO_2 in the upper atmosphere, J. Geophys. Res., 117, D05305, doi:10.1029/2011JD016933, 2012.

Schuck, T. J., Brenninkmeijer, C. A. M., Baker, A. K., Slemr, F., von Velthoven, P. F. J., and Zahn, A.: Greenhouse gas relationships in the Indian summer monsoon plume measured by the CARIBIC passenger aircraft, Atmos. Chem. Phys., 10, 3965–3984, doi:10.5194/acp-10-3965-2010, 2010.

Spivakovsky, C. M., Logan, J. A., Montzka, S. A., Balkanski, Y. J. Foreman-Fowler, M., Jones, D. B. A., Horowitz, L. W., Fusco, A. C. Brenninkmeijer, C. A. M., Prather, M. J., Wofsy, S. C., and McElroy, M. B.: Three-dimensional climatological distribution of tropospheric OH: update and evaluation, J., Geophys. Res., 105, 8931–8980, 2000.

Steele, L. P., Fraser, P. J., Rasmussen, R. A., Khalil, M. A. K., Conway, T. J. Crawford, A. J., Gammon, R. H., Masarie, K. A., and Thoning, K. W.: The global distribution of methane in the troposphere, J. Atmos. Chem., 5, 125–171, 1987.

Sudo, K., Takahashi, M., Kurokawa, J., and Akimoto, H.: CHASER: a global chemical model of the troposphere. 1. Model description, J. Geophys. Res., 107, 4339, doi:10.1029/2001JD001113, 2002.

Sugawara, S., Nakazawa, T., Inoue, G., Machida, T., Mukai, H., Vinnichenko, N. K., and Khattatov, V. U.: Aircrat measurements of the stable carbon isotopic ratio of atmospheric methane over Siberia, Global Biogeochem. Cy., 10, 223–231, 1996.

Sugawara, S., Nakazawa, T., Shirakawa, Y., Kawamura, K., Aoki, S., Machida, T., and Honda, H.: Vertical profile of the carbon isotopic ratio of stratospheric methane over Japan, Geophys. Res. Lett., 24, 2989–2992, 1997.

Takigawa, M., Takahashi, M., and Akiyoshi, H.: Simulation of ozone and other chemical species using a Center for Climate System Research/National Institute for Environmental Studies atmospheric GCM with coupled stratospheric chemistry, J. Geophys. Res., 104, 14003–14018, 1999.

Tanaka, M., Nakazawa, T., and Aoki, S.: Concentrationof atmospheric carbon dioxide over Japan, J. Geophys. Res., 88, 1339–1344, 1983.

ACPD

12, 9035–9077, 2012

Tanaka, M., Nakazawa, T., and Aoki, S.: Time and space variations of tropospheric carbon dioxide over Japan, Tellus B, 39, 3–12, 1987a.
Tanaka, M., Nakazawa, T., and Aoki, S.: Seasonal and meridional variations of atmospheric carbon dioxide in the lower troposphere of the Northern and Southern Hemispheres, Tellus B, 39, 29–41, 1987b.
Terao, Y., Mukai, H., Nojiri, Y., Machida, T., Tohjima, Y., Saeki, T., and Maksyutov, S.: Interannual variability and trends in atmospheric methane over the Western Pacific from 1994 to 2010, J. Geophys. Res., 116, D14303, doi:10.1029/2010JD015467, 2011.
Tohjima, Y., Machida, T., Utiyama, M., Katsumoto, M., Fujinuma, Y., and Maksyutov, S.: Analysis and presentation of in situ atmospheric methane measurements from Cape Ochi-ishi and Hateruma Island, J. Geophys. Res., 107, 4148, doi:10.1029/2001JD001003, 2002.
Tyler, S. C., Ajie, H. O., Gupta, M. L., Cicerone, R. J., Blake, D. R., and Dlugolencky, E. J.: Stable carbon isotopic composition of atmospheric methane: a comparison of surface level and free tropospheric air, J. Geophys. Res., 104, 13895–13910, 1999.
Tyler, S. C., Ajie, H. O., Rice, A. L., Cicerone, R. J., and Tuazon, E. C.: Experimentally determined kinetic isotope effects in the reaction of CH_4 with Cl: implications for atmospheric CH_4, Geophys. Res. Lett., 27, 1715–1718, 2000.
Tyler, S. C., Rice, A. L., and Ajie H. O.: Stable isotope ratios in atmospheric CH_4: implications for seasonal sources and sinks, J. Geophys. Res., 112, D03303, doi:10.1029/2006JD007231, 2007.
Umezawa, T.: A study of global methane cycle based on measurements of its carbon and hydrogen isotopes in the atmosphere, Ph.D. thesis, Graduate school of science, Tohoku University, Sendai, Japan, 2009.
Umezawa, T., Aoki, S. Morimoto, S., and Nakazawa, T.: A high-precision measurement system for carbon and hydrogen isotopic ratios of atmospheric methane and its application to air samples collected in the Western Pacific region, J. Meteorol. Soc. Jpn., 87, 365–379, 2009.
Umezawa, T., Aoki, S. Kim, Y. Morimoto, S., and Nakazawa, T.: Carbon and hydrogen stable isotopic ratios of methane emitted from wetlands and wildfires in Alaska: aircraft observations and bonfire experiments, J. Geophys. Res., 116, D15305, doi:10.1029/2010JD015545, 2011.
Xiong, X., Houweling, S., Wei, J., Maddy, E., Sun, F., and Barnet, C.: Methane plume over south Asia during the monsoon season: satellite observation and model simulation, Atmos. Chem. Phys., 9, 783–794, doi:10.5194/acp-9-783-2009, 2009.

ACPD
12, 9035–9077, 2012

Yamaji, K., Ohara, T., and Akimoto, H.: A country-specific, high-resolution emission inventory for methane from livestock in Asia in 2000, Atmos. Environ., 37, 4393–4406, 2003.
Yan, X., Ohara, T., and Akimoto, H.: Development of region-specific emission factors and estimation of methane emission from rice fields in the East, Southeast and South Asian countries, Glob. Change Biol., 9, 237–254, 2003.
Yashiro, H., Sugawara, S. Sudo, K., Aoki, S., and Nakazawa, T.: Temporal and spatial variations of carbon monoxide over the western part of the Pacific Ocean, J. Geophys. Res., 114, D08305, doi:10.1029/2008JD010876, 2009.
Yoshida, Y., Ota, Y., Eguchi, N., Kikuchi, N., Nobuta, K., Tran, H., Morino, I., and Yokota, T.: Retrieval algorithm for CO_2 and CH_4 column abundances from short-wavelength infrared spectral observations by the Greenhouse gases observing satellite, Atmos. Meas. Tech., 4, 717–734, doi:10.5194/amt-4-717-2011, 2011.
Zhou, L. X., Worthy, D. E. J., Lang, P. M., Ernst, M. K., Zhange, X. C., Wen, Y. P., and Li, J. L.: Ten years of atmospheric methane observations at a high elevation site in Western China, Atmos. Environ., 38, 7041–7054, 2004.
Zhou, L. X., Kitzis, D., and Tans, P. P.: Report of the Fourth WMO Round-Robin Reference Gas Intercomparison, 2002–2007. Report of the 14th WMO Meeting of Experts on Carbon Dioxide Concentration and Related Tracer Measurement Techniques, Helsinki, Finland, 10–13 September 2007, WMO/GAW Rep. 186, T. Laurila, Geneva, Swizerland, 40–43, 2009.

ACPD
12, 9035–9077, 2012

Table 1. Regions assigned for tagged tracer experiments.

No.	Region
1	Europe
2	Western Siberia
3	Eastern Siberia
4	Middle East
5	South Asia
6	East Asia
7	Japan and Korea
8	Southeast Asia
9	Maritime Continent
10	Africa
11	Australia and New Zealand
12	Boreal North America
13	Temperate North America
14	South America
15	Others

ACPD
12, 9035–9077, 2012

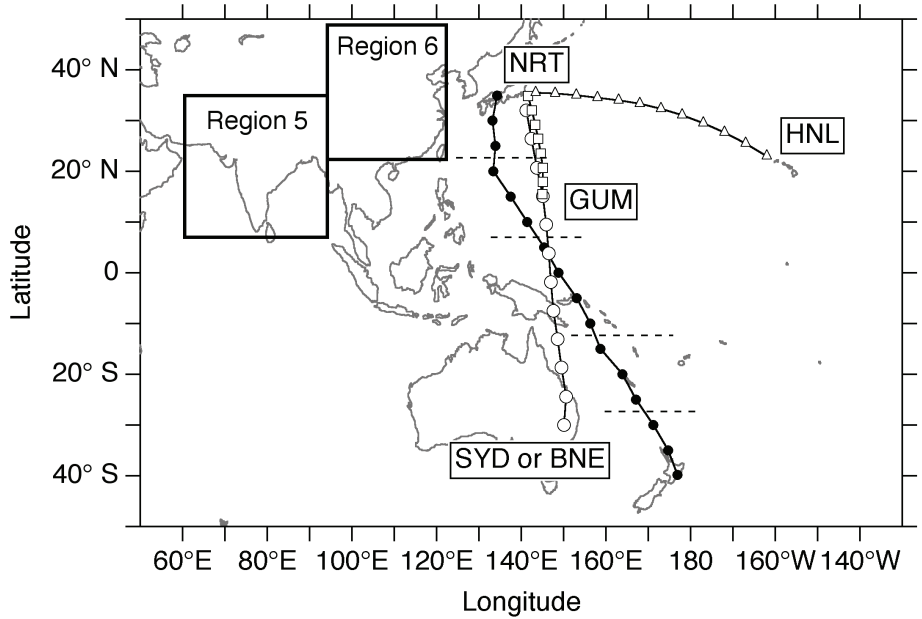

Fig. 1. A map showing locations where air samples were collected in this study. NRT: Narita, GUM: Guam, HNL: Honolulu, SYD: Sydney, BNE: Brisbane. The air sampling was made between NRT and SYD or BNE for December 2005–March 2009 (open circles), between NRT and GUM for April 2009–March 2010 (open squares) and between NRT and HNL for April–September 2010 (open triangles). Also shown are air sampling locations by container ships (closed circles). Dashed lines on the ship track represent the division of latitude bands for the data analysis (see text). Boxes denote the two regions (Region 5 and Region 6) assigned for the tagged experiments.

ACPD
12, 9035–9077, 2012

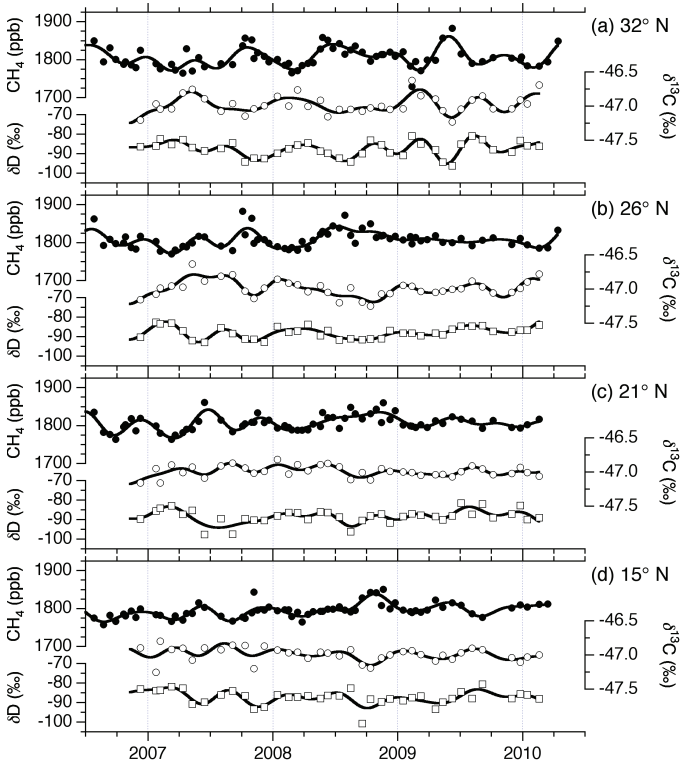

Fig. 2. Temporal variations of the CH_4 mixing ratio (closed circles), $\delta^{13}C$ (open circles) and δD (open squares) in the UT at **(a)** 32° N, **(b)** 26° N, **(c)** 21° N and **(d)** 15° N in the UT between Australia and Japan and between Japan and Guam. Also shown are the best-fit curves to the observed data (solid lines).

ACPD
12, 9035–9077, 2012

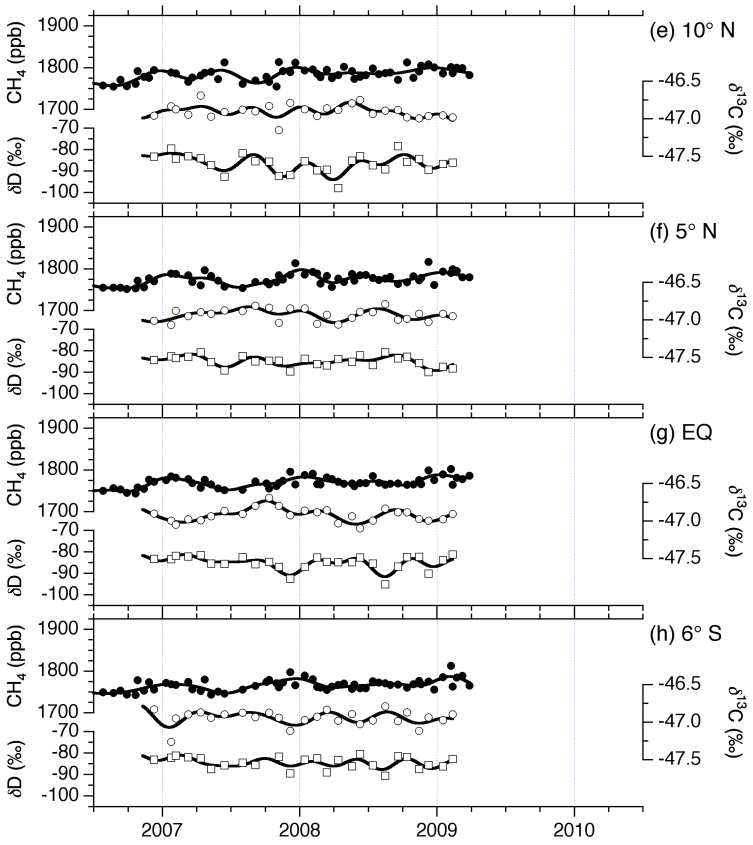

Fig. 2. Same as Fig. 2a–d, but for **(e)** 10° N, **(f)** 5 °N, **(g)** the equator and **(h)** 6° S between Australia and Japan.

ACPD
12, 9035–9077, 2012

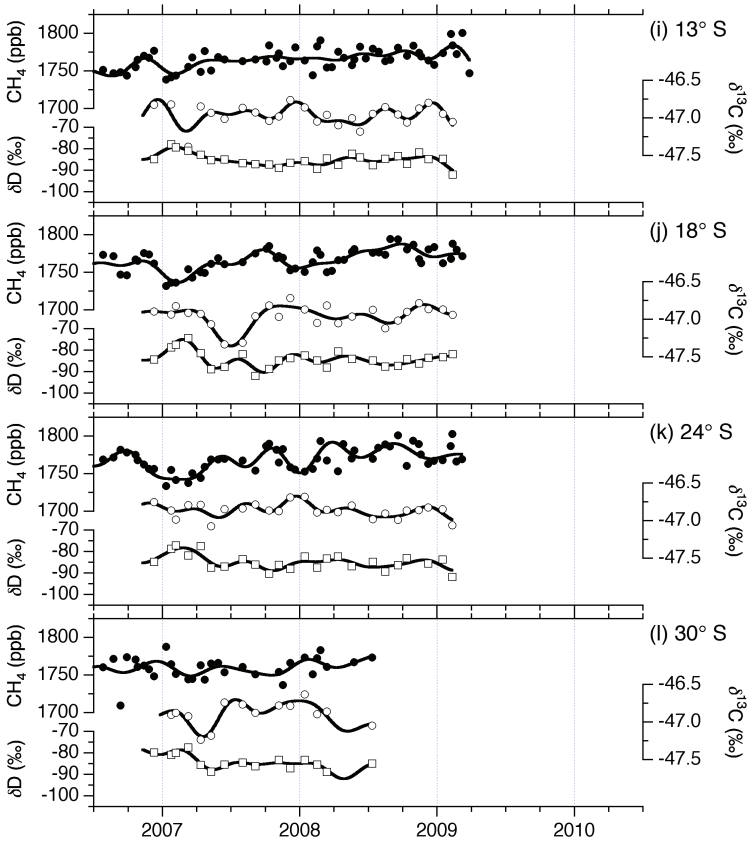

Fig. 2. Same as Fig. 2a–d, but for **(i)** 13° S, **(j)** 18° S, **(k)** 24° S and **(l)** 30° S beween Australia and Japan. Note that the axis ranges of the CH_4 mixing ratio is different from that in Fig. 2a–h.

ACPD
12, 9035–9077, 2012

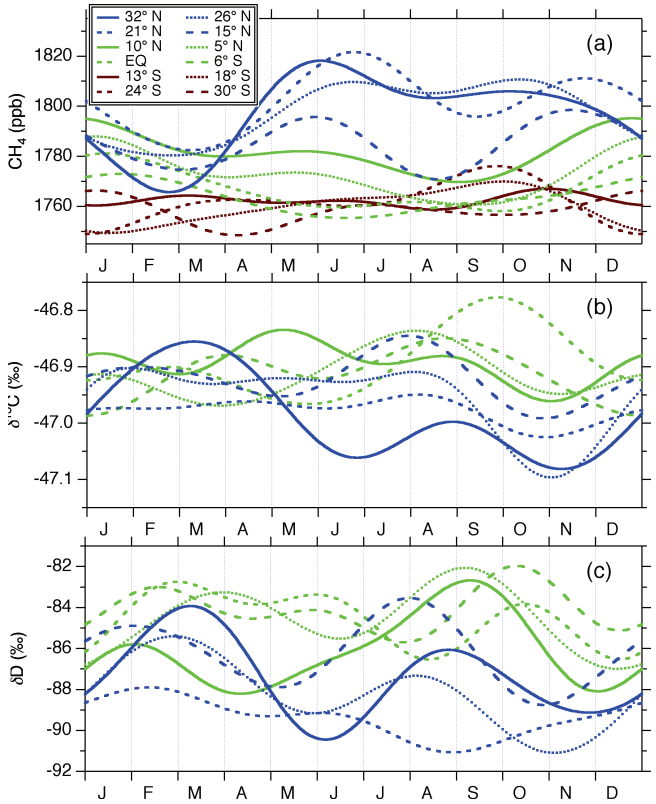

Fig. 3. Seasonal variations of **(a)** the CH_4 mixing ratio, **(b)** $\delta^{13}C$ and **(c)** δD in the NH-UT over the Western Pacific. Each line represents the average seasonal cycle added by the annual average in 2007. Clear seasonal cycles of $\delta^{13}C$ and δD are not observable in the SH and are not shown.

ACPD
12, 9035–9077, 2012

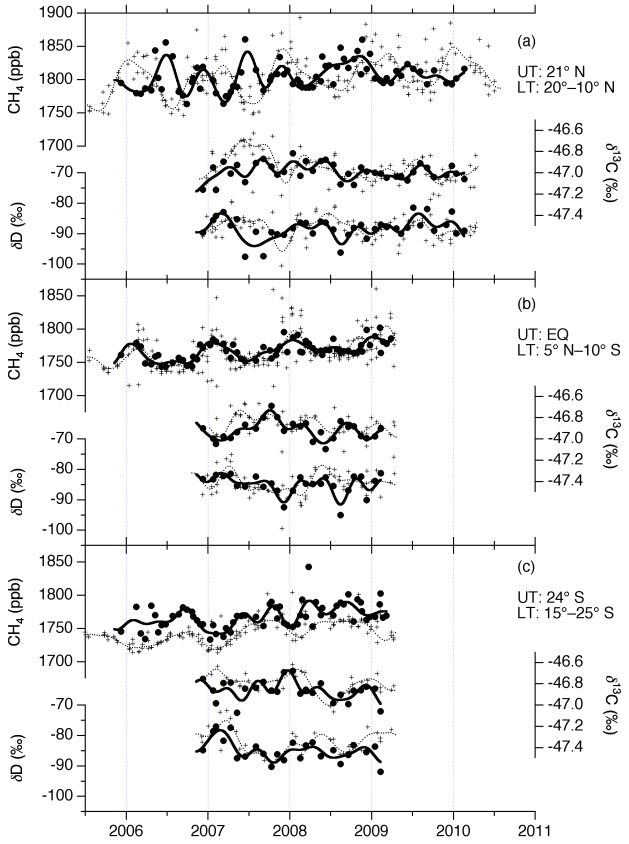

Fig. 4. Variations of the CH_4 mixing ratio, $\delta^{13}C$ and δD in the UT (closed circles) and LT (crosses) over the western Pacific. Also shown are the best-fit curves to the UT (solid line) and LT (dotted line) data.

ACPD
12, 9035–9077, 2012

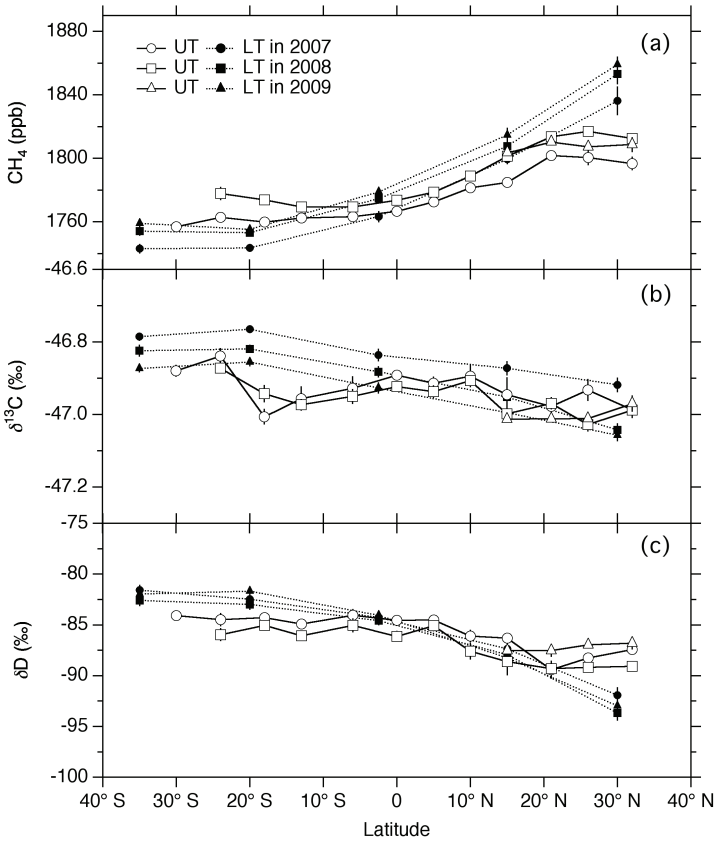

Fig. 5. Latitudinal distributions of annual averages of **(a)** the CH_4 mixing ratio, **(b)** $\delta^{13}C$ and **(c)** δD in the UT (open symbols with solid lines) and LT (closed symbols with dotted lines). Each error bar represents one standard error of the data deviations from the best-fit curves.

ACPD
12, 9035–9077, 2012

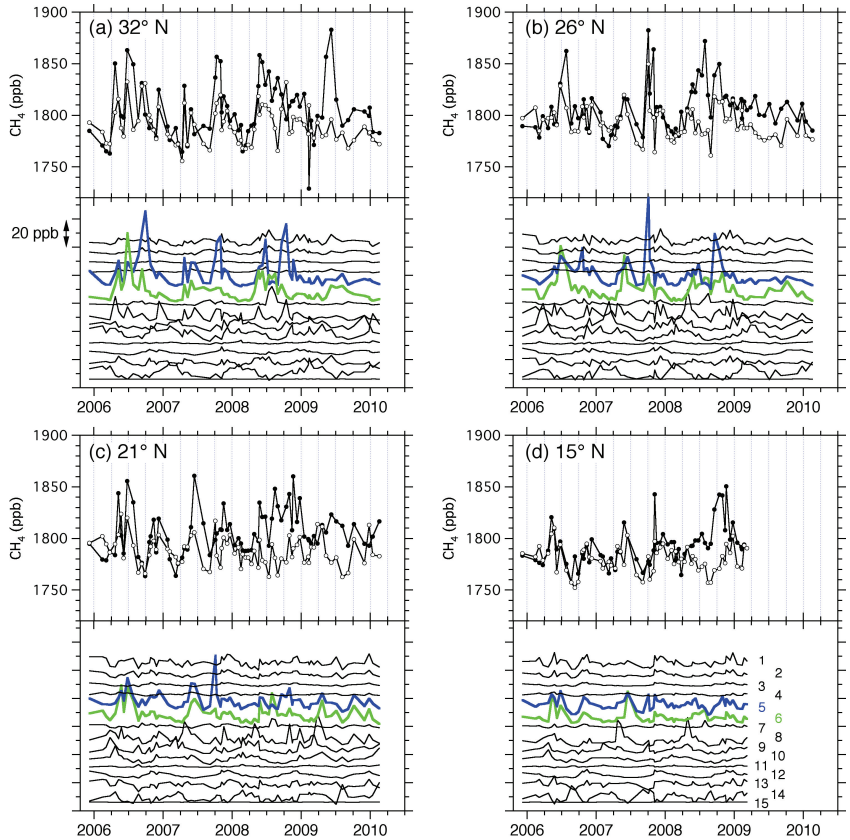

Fig. 6. Comparison of the observed (closed circles) and model-simulated (open circles) CH_4 mixing ratios for the UT at **(a)** 32° N, **(b)** 26° N, **(c)** 21° N and **(d)** 15° N. In each lower panel, shown are the tagged tracers for the respective regions 1–15 (from top to bottom). Blue and green lines represent Region 5 (South Asia) and Region 6 (East Asia), respectively, and each line is offset for easy look.

ACPD
12, 9035–9077, 2012

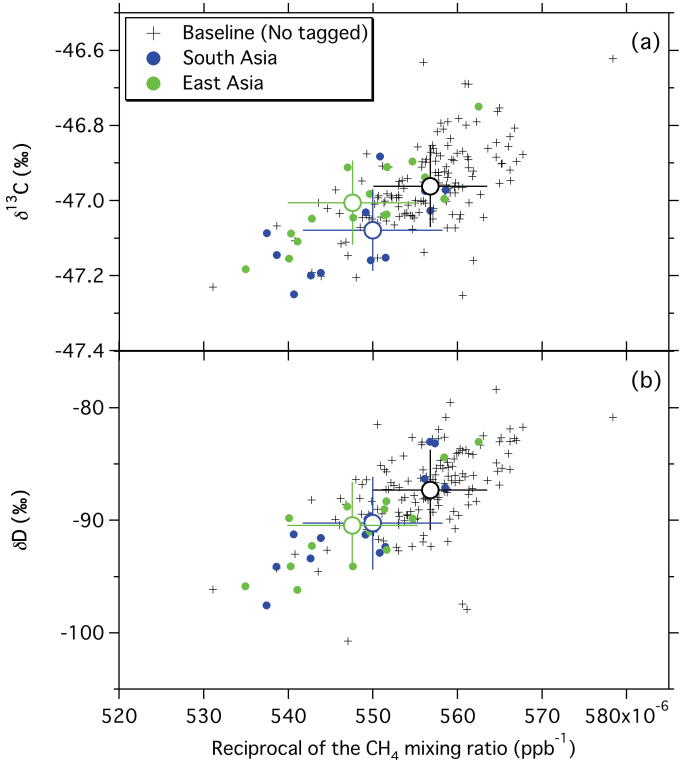

Fig. 7. Plots for **(a)** δ^{13}C and **(b)** δD relative to the reciprocal of the CH_4 mixing ratio for the UT at 15°–32° N. All data plotted were categorized into "Baseline" (black crosses), "South Asia" (blue closed circles) or "East Asia" (green closed circles) based on the tagged tracer experiments. Also shown are the average values of the data for the respective categories (open circles).

ACPD
12, 9035–9077, 2012

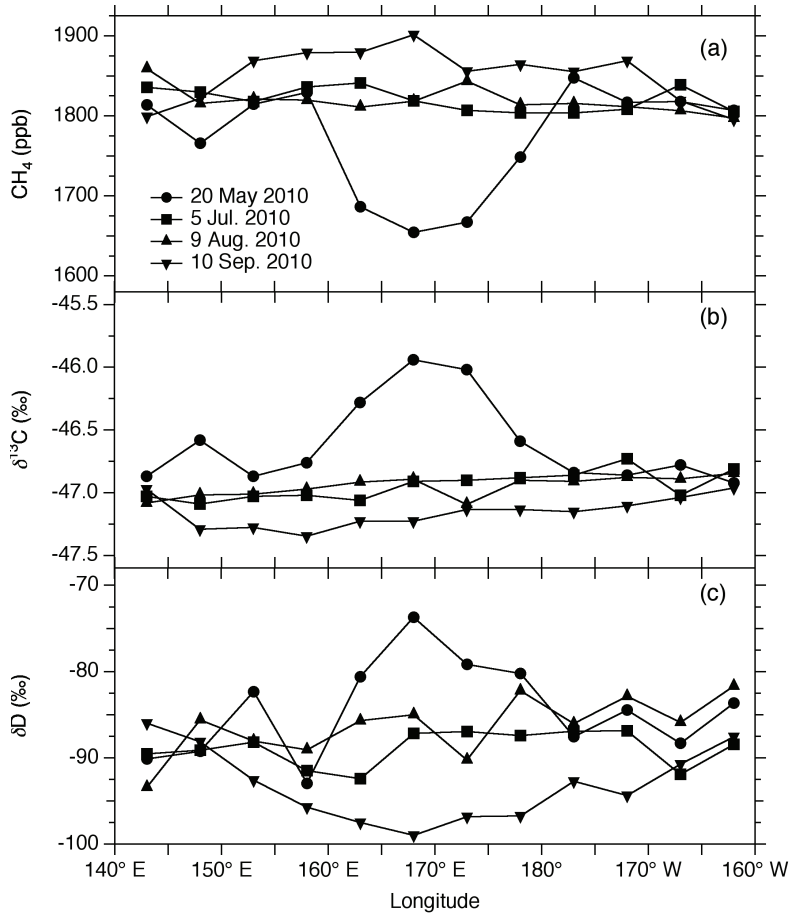

Fig. 8. Longitudinal distributions of **(a)** the CH_4 mixing ratio, **(b)** $\delta^{13}C$ and **(c)** δD observed in four flights between Honolulu, Hawaii and Narita, Japan.

ACPD
12, 9035–9077, 2012